Direct observation of valence transition in $CeNi_{1-x}Co_xSn$ alloys by x-ray and photoelectron spectroscopies

H. Yamaoka,[1] N. Tsujii,[2] K. Yamamoto,[1] H. Oohashi,[3] A. M. Vlaicu,[3] K. Kunitani,[4] K. Uotani,[4] D. Horiguchi,[5] T. Tochio,[6] Y. Ito,[5] and S. Shin[1,7]

[1]*Harima Institute, RIKEN (The Institute of Physical and Chemical Research), Sayo, Hyogo 679-5148, Japan*

[2]*Quantum Beam Center, National Institute for Materials Science, 1-2-1 Sengen, Tsukuba 305-0047, Japan*

[3]*Harima Office, National Institute for Materials Science, Sayo, Hyogo 679-5148, Japan*

[4]*Department of Engineering, Okayama University, Okayama 700-8530, Japan*

[5]*Institute for Chemical Research, Kyoto University, Uji, Kyoto 611-0011, Japan*

[6]*Keihanna Interaction Plaza Incorporated, Kyoto 619-0237, Japan*

[7]*Institute of Solid State Physics, University of Tokyo, Kashiwa, Chiba 277-85817, Japan*

(Received 1 May 2007; published 29 August 2007)

We investigated the electronic structure of $CeNi_{1-x}Co_xSn$ ($x=0.33$ and 0.38) as a function of temperature, combining x-ray absorption spectroscopy in the partial fluorescence yield, resonant x-ray emission spectroscopy, and photoelectron spectroscopy. The three spectroscopic techniques provided complementary and consistent information. For $x=0.33$, the valence transition into a mixed-valence regime is deduced to take place around 60 K, as seen from the enhancement of the f^0 and f^2 components and the relative suppression of the f^1 component. The valence was stable for $x=0.38$ for temperatures down to 17 K. The resonant inelastic x-ray scattering was also performed for $x=0.33$ at 17 K, suggesting localized or partially delocalized f states. Kondo peak was observed in the resonant valence spectra, showing the existence of the c-f hybridization. The mechanism of the valence transition is discussed.

DOI: 10.1103/PhysRevB.76.075130 PACS number(s): 75.30.Mb, 61.10.Ht, 71.20.Eh, 78.70.Ck

I. INTRODUCTION

Heavy-fermion behavior exhibited by some rare-earth metals and compounds is accompanied by astonishing physical phenomena, among which is the valence transition at low temperature as observed in Ce metal across the $\alpha \rightarrow \gamma$ transition.[1–5] Such a valence instability is characterized by the formation of a narrow band corresponding to the c-f hybridization between the $4f$ electrons and the conduction band states.

Some models have been proposed to explain such a mechanism of valence transition. Among them, the promotional model assumed a change in the electronic configuration from $4f^1c^3$ to $4f^0c^4$, where c represents conduction electrons.[6,7] Experimental results using photoemission and x-ray absorption, however, revealed that the number of $4f$ electrons does not change significantly through the transition.[4] The Mott transition (MT) model assumed that the $4f$ state is localized in the γ phase but itinerant in the α phase, and is described by band theory. The transition from the γ to the α phase was described by a change in Coulomb repulsion between the $4f$ electrons in the same atom, but photoemission results showed only a small change in the Coulomb repulsion. Later on, Johansson employed local density approximation (LDA) calculations to correct the MT scenario with great success.[8,9] The Kondo volume collapse (KVC) scenario based on the Anderson impurity model was also proposed.[2–5] In the KVC model, the magnetic character is governed by the Kondo temperature T_K, which is related to the hybridization of f^0 in the ground state, and the driving force of the phase transition is the rapid change in T_K due to the volume change.

In the KVC picture, three distinct peaks should be observed in the photoelectron spectrum for both phases of Ce metal: the Kondo (or Abrikosov-Suhl) resonance peak (f^1), corresponding to the Kondo screening by the valence electrons, and the two Hubbard sideband peaks (lower band f^0 and upper band f^2). The KVC model predicts that the Kondo resonance increases drastically at the transition from the γ to the α phase. The α phase of Ce in the KVC model is strongly correlated but not in the MT model. The LDA calculation with dynamical mean-field theory (DMFT) showed that the phase transition is due to the volume change.[10] The LDA+DMFT calculations suggest that α-Ce is strongly correlated to a three-peak structure in the photoelectron spectrum as predicted by the KVC model. These features in the Ce $\alpha \rightarrow \gamma$ transition have been directly observed by the resonant x-ray emission spectroscopies,[11,12] which provided convincing support for the application of the KVC model to Ce.

A similar valence transition has also been discovered in several compounds such as $YbInCu_4$ (Ref. 13) and $YbIn_{1-x}Ag_xCu_4$.[14] The KVC picture was applied to explain the transition of $YbInCu_4$.[15] However, Cornelius *et al.* showed[14] that the KVC model is not applicable because the volume change $\Delta V/V$ at the transition is too small compared to the prediction of the KVC model. Instead, they noted that the small carrier density in the high-temperature phase is relevant to the transition in $YbIn_{1-x}Ag_xCu_4$. In the mixed valence state, the electron is transferred from the conduction band to the Yb $4f$ shell. If the electron transfer lowers the Fermi level in the density of state, the hybridization becomes stronger and the Kondo temperature increases.

Another candidate for the valence transition is $CeNi_{1-x}Co_xSn$,[16] a variation from the well-known Kondo semiconductor CeNiSn.[17–23] By substituting Co to Ni, Adroja *et al.* discovered a sharp drop in the magnetic susceptibility and the resistivity around 30–50 K for $x=0.38$.[16,24,25] While

no magnetic or symmetric transition is observed with neutron diffraction, the lattice constant changes drastically through the transition. From these results, Adroja *et al.* suggested that a valence transition similar to the transition seen in $YbInCu_4$ occurs in $CeNi_{1-x}Co_xSn$, with $x \sim 0.38$. NMR study for the $x=0.35$ sample indicated a transition from a localized $4f$ state at high temperature to the Fermi liquid at low temperature.[26]

In the $CeNi_{1-x}Co_xSn$ system, only a few percent difference in the Co concentration causes a significant change at the transition temperature and a systematic variation in the low-temperature properties. The volume change at the transition is very small, and Adroja *et al.* suggested that the KVC picture may not be suitable.[27] They considered that the fine tuning of the Fermi level due to the substitution may be responsible for the transition, as suggested for $YbInCu_4$.

Substitution of Ni ($3d^8$) by Co ($3d^7$) corresponds to hole doping of the conduction band. The carrier is added to the quasiparticle band by c-f hybridization. The density of state increases due to the doping. Thus it is expected that the Co doping increases the c-f hybridization strength, causing the strongly hybridized state at low temperature. This scenario could be confirmed through the use of x-ray spectroscopies, since, as mentioned above, these have previously yielded conclusive results for the understanding of the microscopic origin of the valence transition in Ce metal.

In this paper, we probe the electronic properties of $CeNi_{1-x}Co_xSn$ ($x=0.33$ and 0.38) through the valence transition by means of x-ray absorption spectroscopy in the partial fluorescence yield mode (PFY-XAS), resonant x-ray emission spectroscopy (RXES), and resonant photoelectron spectroscopy (RPES). The results obtained by PFY-XAS and RXES provide clear evidence of the valence change for $x=0.33$ around 60 K. Besides, we investigate the change in the c-f hybridization strength by high-resolution x-ray photoelectron spectroscopy and discuss the origin of the valence transition in $CeNi_{1-x}Co_xSn$. The PFY-XAS and RXES including resonant inelastic x-ray scattering (RIXS) provide information on the bulk electronic properties. The RPES shows the electronic state near the Fermi edge. We employed these methods to obtain complementary information.

II. EXPERIMENTS

A. Samples

Polycrystalline samples were prepared by argon arc melting from pure metals. The $CeNi_{1-x}Co_xSn$ samples ($x=0.32$, 0.33, 0.34, 0.36, 0.38, and 0.40) were subsequently annealed in evacuated silica tubes at 1000 °C for two weeks. We also have an as-cast sample of $x=0.33$ without annealing, which shows less drastic change in the temperature dependence of the magnetic susceptibility compared to the annealed one. The samples, used for x-ray emission and photoelectron spectroscopies, were taken from the same rods. The magnetic susceptibility was measured with a superconducting quantum interference device magnetometer (Quantum Design, MPMS5S).

We used an Iwatani CRT-M310-OP cryostat (lowest temperature of about 17 K) to cool down the samples. In accordance with the capability of the cryostat, we chose two samples with $x=0.33$ (as-cast) and $x=0.38$ for the spectroscopic measurements.

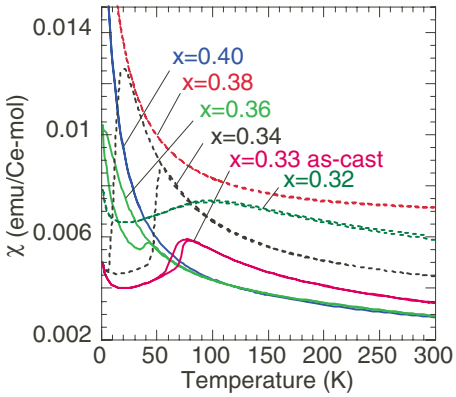

FIG. 1. (Color online) Temperature dependence of the magnetic susceptibility of $CeNi_{1-x}Co_xSn$.

B. X-ray emission spectroscopy

The resonant x-ray emission and absorption spectroscopy measurements were performed at the BL15XU undulator beamline of SPring-8.[28] The undulator beam was monochromatized by a water-cooled double crystal monochromator. The energy calibration of the beamline monochromator was performed with the K absorption edge of reference metals. X-ray emission was measured with a Ge 111 double crystal spectrometer with (+, +) geometry.[29] The Ge 111 lattice constant had been estimated before[30] and the energy calibration of the spectrometer was performed by the using Ce $L\alpha_1$ line. The resolution $E/\delta E$ (E, photon emission energy) was estimated to be about 3350 at 8050 eV without solar slit system. Finally, thanks to the top-up operation of the SPring-8 storage ring, we had a very stable incident photon beam.[31]

C. Photoelectron spectroscopy

Photoelectron spectroscopy measurements were performed at the BL17SU soft x-ray undulator beamline of SPring-8 (Refs. 32 and 33) with a hemispherical electron analyzer SCIENTA SES 2002.[34] During the measurement, the vacuum pressure was kept below $(2-3)\times 10^{-8}$ Pa. In every measurement, we confirmed that the sample is free from oxygen contamination by monitoring the oxygen signal. Au $4f$ lines were used to correct the measured photoelectron energy in every measurement when the incident photon energy was changed. The resolution δE (E, photoelectron energy) of the analyzer was estimated from the Au Fermi edge to be 95 meV for the high-resolution case and 170 meV for the low-resolution case.

III. RESULTS AND DISCUSSION

A. Magnetic susceptibility

Figure 1 shows the temperature dependence of the mag-

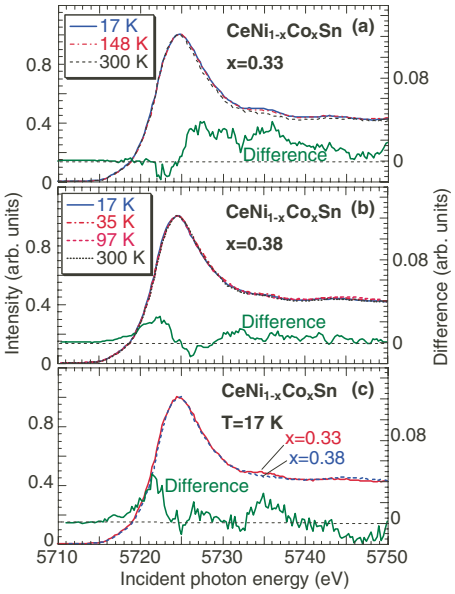

FIG. 2. (Color online) Temperature dependence of the PFY of $CeNi_{1-x}Co_xSn$: (a) $x=0.33$ as-cast, (b) $x=0.38$ samples with the difference spectra between 17 and 300 K, and (c) the comparison between $x=0.33$ and 0.38 at 17 K.

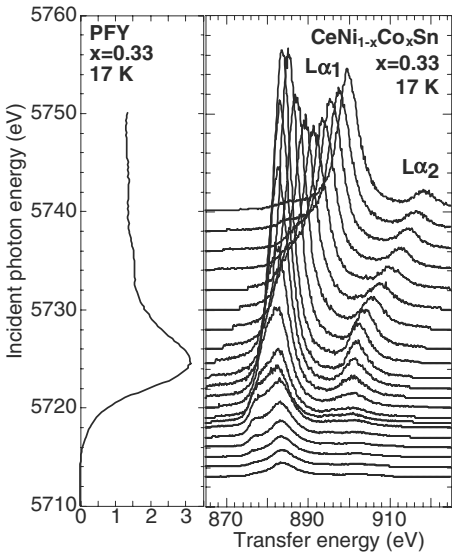

FIG. 3. Resonant inelastic scattering spectra for $x=0.33$ at 17 K with the PFY spectrum as a function of the incident photon energies.

netic susceptibility of $CeNi_{1-x}Co_xSn$. Above $x=0.38$, the magnetic susceptibility follows the Curie-Weiss law. On the other hand, the sample with $x=0.32$ shows a typical mixed-valence behavior. Within a narrow range ($0.34 \leqslant x \leqslant 0.36$), the samples show a strong deviation from the Curie-Weiss law and possibility of valence change. These samples show a sharp drop in susceptibility with a large hysteresis behavior, consistent with the previous report by Adroja *et al.*[27] An as-cast unannealed sample ($x=0.33$) also shows a similar transition but with less prominent hysteresis. Adroja *et al.* found similar characteristics although there is a small shift for the Co concentration x dependence and the values of the magnetic susceptibilities are slightly different.[16] In our spectroscopic measurements, we focused on the study of two samples: $x=0.33$ (as-cast) and $x=0.38$.

B. X-ray absorption spectroscopy

Figure 2 shows the PFY-XAS spectra measured at several temperatures for $x=0.33$ (as-cast) and 0.38. We show the differences of the intensities between 17 and 300 K in Figs. 2(a) and 2(b), and that between $x=0.33$ and 0.38 at 17 K in Fig. 2(c). The emission energy of the spectrometer was tuned to the peak of the Ce $L\alpha_1$ ($3d_{5/2} \rightarrow 2p_{3/2}$) emission line and the incident photon energy is scanned through the Ce L_3 edge. The obtained spectra display features with higher resolution than conventional absorption.[30] The spectra are normalized to the intensity of the maximum of the white line. In mixed-valence Ce compounds, Ce can be in three different electronic states, $4f^0$ (4+), $4f^1$ (3+), and $4f^2$ (2+).[35] The PFY-XAS process for each of these valences corresponds to the following respective transitions between the initial, intermediate, and final states (similar to RXES): $4f^0 \rightarrow 2p^5 4f^0 5d \rightarrow 2p^6 3d^9 4f^0 5d$, $4f^1 \rightarrow 2p^5 4f^1 5d \rightarrow 2p^6 3d^9 4f^1 5d$, and $4f^2 \rightarrow 2p^5 4f^2 5d \rightarrow 2p^6 3d^9 4f^2 5d$. As seen in Fig. 2, these components are respectively located around 5720 eV (hidden in the low energy tail of the $4f^1$ peak[35]), the white line maximum, and 5735 eV.

The temperature dependence of the magnetization for $x=0.33$ (Fig. 1) suggests a small change in the valence around 60 K, compared to the Ce metal case. However, the PFY-XAS spectra in Fig. 2 clearly show the temperature dependence for $x=0.33$, while there is almost no dependence for $x=0.38$. For $x=0.33$ at 17 K, the intensity of f^0 increases, signifying the increase of the valence. The mean valence of $x=0.33$ at 17 K is estimated to be about 3.01 from the curve fit for the PFY-XAS spectrum when the hidden and small f^2 contribution is ignored. Figure 2(c) shows the difference between the spectra of $x=0.33$ and 0.38 at 17 K. These results clearly show relative enhancement of the f^0 and f^2 components for $x=0.33$, and therefore, an increase in the $4f$ hybridization strength. We note that our results show a change in the $4f$ occupation number for $x=0.33$ about ten times smaller than in the case of the γ to α transition in Ce metal (from 0.95 to 0.85).[11]

C. Resonant x-ray emission spectroscopy

RXES spectra measured for several incident energies across the Ce L_3 edge (RIXS) are shown in Fig. 3 along with the PFY-XAS spectrum for $x=0.33$ at 17 K. The intensities are normalized by the incident beam intensities. We can observe the Raman component around the absorption edge and the fluorescence above the edge.[36] The Raman scattering does not change with the transfer energy, whereas the fluorescence energy is proportional to the transfer energy.[30,37–41] We used the same curve fitting procedure as for the Eu system[30] to separate the Raman component, which is directly related to the valence electronic states, from the $L\alpha$ fluorescence signal.

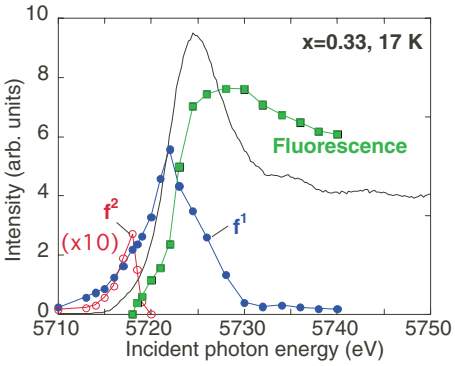

FIG. 4. (Color online) f^1, f^2, and fluorescence components as a function of the incident photon energies with the PFY spectrum. The intensity of f^2 is small and the vertical scale for f^2 is ten times as large as the scale of the other components.

Figure 4 shows the results of the curve fitting for the RIXS spectra in Fig. 3 as a function of the incident photon energies. It consists mainly of f^1 (3+) with a small fraction of f^2 (2+). The intensity of f^2 to f^1 is estimated to be 1.7% from Fig. 4. In our system, there is no pre-edge peak. We find that the Raman regime vanishes at an energy as high as around 5730 eV, almost 10 eV above the absorption edge. One can, therefore, say that the $4f$ state retains the localized character or is partially delocalized and, thus, the hybridization may not be strong.[43]

Annese *et al.* showed the small contribution of the quadrupole component in Yb L_3 XAS spectra of YbS.[42] In our case, in the XAS and Ce $L\alpha$ emission spectra in Figs. 3 and 5, we do not observe this component clearly. The contribution of the quadrupole component may be small and, thus, we ignore the quadrupole contribution in the analyses.

In the PFY-XAS spectrum, each component is modeled by the sum of an arctangent (continuum excitation) and voigt

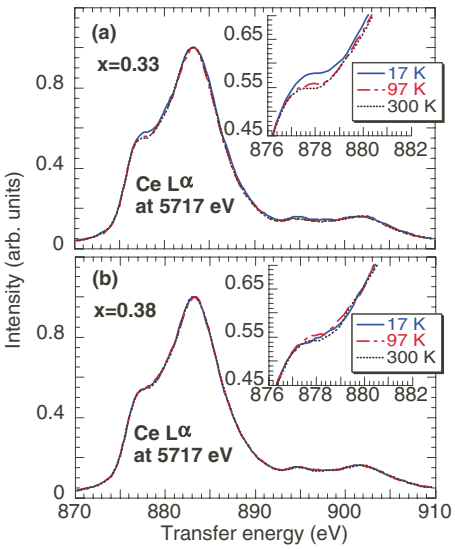

FIG. 5. (Color online) Temperature dependence of Ce $L\alpha_1$ emission at the incident photon energy of 5717 eV for $CeNi_{1-x}Co_xSn$ (x=0.33 and 0.38). Insets show enlarged parts of the $4f^2$ shoulder. The intensity is normalized to the maximum of the f^1 component.

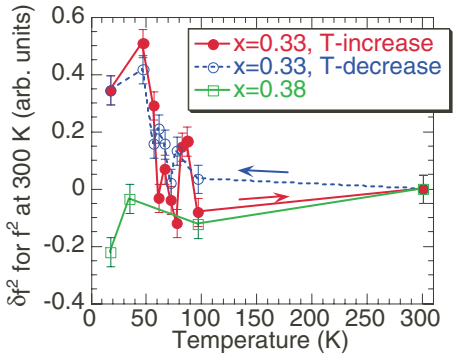

FIG. 6. (Color online) Relative intensity change in f^2 as a function of the temperature compared to the intensity at 300 K.

(white peak) functions. The continuum part greatly contributes to the uncertainty, so we only considered the white line region to estimate the respective intensity of each component. In the PFY spectrum, it is difficult to fit the small intensity of f^2, and the intensity ratio of f^1 to f^0 is 1% for x=0.33 at 17 K. By combining the results of RIXS and PFY, we can estimate the intensity ratio of each component, $f^0:f^1:f^2=0.97:97.4:1.62$, where $f^0+f^1+f^2=1$. It is noted that in Ce compounds there is normally hybridization among the f^n states and, thus, the above intensity ratio does not show the exact valence ratio. We can, however, compare the relative change in the valence qualitatively. At low temperature after the valence transition in x=0.33, the f^1 component decreases by 2%–3%, while the f^0 and f^2 increase by 1%–2%.

Figure 5 shows the temperature dependence of the Ce $2p$-$3d$ RXES spectrum obtained for x=0.33 and 0.38 at an incident photon energy of 5717 eV, where the fluorescence component can be ignored as shown in Fig. 4. The spectra intensity is normalized to the maximum of the f^1 component. The horizontal axis is the transfer energy, defined as the difference between the incident photon energy and the emission energy. The spectrum consists of the $L\alpha_1$ ($2p_{3/2}$-$3d_{5/2}$) and $L\alpha_2$ ($2p_{3/2}$-$3d_{3/2}$) emissions. The two peaks at 877 and 883 eV correspond respectively to the f^2 and f^1 components; the $2p^64f^2 \rightarrow 2p^54f^25d \rightarrow 2p^63d^94f^25d$ and $2p^64f^1 \rightarrow 2p^54f^15d \rightarrow 2p^63d^94f^15d$ transitions. Therefore, the final states of f^1 and f^2 in Fig. 5 represent the weight of the f^1 and f^2 components in the initial states, respectively. The spectrum obtained for x=0.33 shows an increase of the relative intensity of the f^2 feature as the temperature is decreased, which we interpret here as the relative decrease of the $4f^1$ component.

In Fig. 5, the change in the f^2 intensity is not large and it is not easy to see such a small difference in exact curve fit. Thus, we simply compare the differences, δf^2 [$=I(T)-I(300)$], between the area of f^2 at 872–882 eV at a given temperature [$I(T)$] and that at 300 K [$I(300)$]. Figure 6 shows the relative intensity change in δf^2 as a function of temperature. In Fig. 5, we normalized the intensity to the intensity of f^2. Thus, the relative change in the intensity of f^2 in Fig. 6 is considered to be the change in the intensity of f^1, although in Fig. 6 we only show the change in f^2. For the

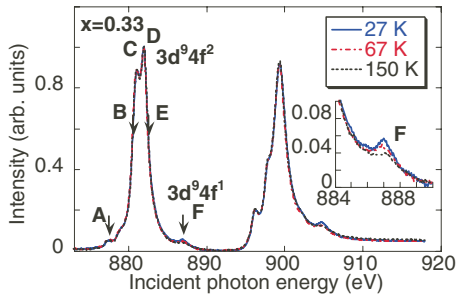

FIG. 7. (Color online) Absorption spectra (total electron yields) for $x=0.33$ at 27, 67, and 150 K. The RPES is performed at the energies indicated by the arrow as will be shown later in Fig. 10.

$x=0.33$ sample, we measured the spectra by decreasing and increasing the temperature because hysteresis is observed in the measurement of the susceptibility. δf^2 for the $x=0.33$ sample shows a sudden change between 50 and 70 K compared to the case for the $x=0.38$ sample, corresponding to the trend in the temperature dependence of the susceptibility. δf^2 for $x=0.38$ is relatively stable for temperatures down to 17 K. These results show clear and direct evidence of the valence transition around 60 K for the $x=0.33$ sample. A similar trend has also been observed in Ce metal[12] and Ce alloys.[11] We also measured the $L\alpha$ emission spectra as a function of temperature at the incident energies of 5718.5, 5724.5, and 5736 eV, but no temperature dependence was observed. We believe that this is due to the concomitant relative decrease of f^2 and increase of the fluorescence components which compensate each other at these incident energies.

D. Resonant photoelectron spectroscopy

The Ce $3d$-$4f$ ($M_{4,5}$) absorption spectra (total electron yields) for $x=0.33$ are shown in Fig. 7 as a function of the temperature, after subtracting a constant background. The samples were taken from the same rods used for x-ray emission spectroscopy. Two main peaks at about 882 and 900 eV correspond to the $4f^1 \rightarrow 3d^9f^2$ transition. In the Ce system, it is known that the valence mixing in the ground state is represented by the satellite peaks at 887 and 905 eV in the final states ($3d^9f^1$ in Fig. 7). The transition is $4f^0 \rightarrow 3d^9f^1$, and $3d^9f^1$ represents the weight of the f^0 component in the initial state.[12,44,45] The results show that the f^0 component increases as the temperature decreases for $x=0.33$.

The Ce $3d$ photoelectron spectra for $x=0.33$ and 0.38 at 27 and 155 K, at the incident photon energy of 1500 eV, are shown in Fig. 8. As mentioned before, these samples and the samples used in the photon emission spectroscopy were taken from the same rods. The assignment is well known: the main peaks are $3d_{3/2}$ and $3d_{5/2}$, respectively, and the additional peak at 870 eV is due to Ni $2p_{3/2}$.[46] f^0, f^1, and f^2 in Fig. 8 correspond respectively to the $4f^0 \rightarrow 3d^9 4f^0 \underline{\epsilon}$, $4f^1 \rightarrow 3d^9 4f^1 \underline{\epsilon}$, and $4f^2 \rightarrow 3d^9 4f^2 \underline{\epsilon}$ transitions. The final states of f^0, f^1, and f^2 in Fig. 8 represent respectively the weight of the f^0, f^1, and f^2 components in the initial states.

For $x=0.33$, the f^1 component decreases as the temperature decreases, whereas for $x=0.38$, there is almost no

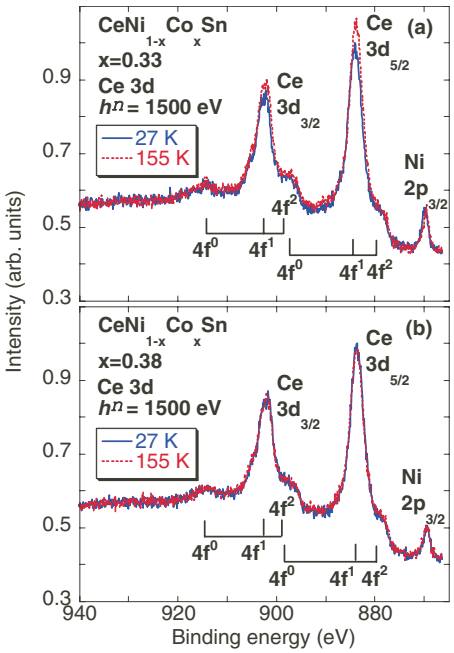

FIG. 8. (Color online) Ce $3d$ photoelectron spectra for $x=0.33$ and 0.38 at 27 and 155 K at the incident photon energy of 1500 eV. The energy positions of f^n are conventionally assigned (not the calculated ones).

change. The intensity of f^1 for $x=0.33$ at 67 K is not shown in Fig. 8 because it is between the intensities at the temperatures of 27 and 155 K. The decrease of f^1 is interpreted as an increase of f^0 in the ground state.[46] Curve fit for the data in Fig. 8 gives the intensity ratio of each component, $f^0:f^1:f^2 = 2.26:93.9:3.82$ for $x=0.33$ at 27 K and $f^0:f^1:f^2 = 1.68:94.8:3.48$ for $x=0.33$ at 155 K, where $f^0+f^1+f^2=1$. It is noted that the photoemission spectroscopy (PES) at 1500 eV is still surface sensitive, while, on the other hand, RXES is essentially bulk sensitive. This may be a reason why the ratios obtained with the PES are slightly different from those obtained with the RXES and PFY-XAS, although the trend is the same. These results from Figs. 7 and 8 show that for the $x=0.33$ sample, f^0 increases by 0.5%–0.6% after the phase transition when the temperature decreases.

Figure 9 shows the nonresonant valence spectra for $x=0.33$ and 0.38 at the incident photon energy of 800 eV as a function of the temperature. There is almost no temperature dependence. We also show an example of the effect of the contamination by oxygen for the $x=0.38$ sample in Fig. 9(b). As noted before, during the measurement, we always checked the oxygen photoelectron peak to avoid the contamination. We measured Sn $3d$ photoelectron spectra at the incident photon energy of 1500 eV as a function of the temperature, but we found no change. We cannot observe the temperature dependence in the nonresonant valence spectra.

Therefore, we measured the Ce $3d$-$4f$ resonant photoelectron spectra (Fig. 10). The enlarged spectra at the Fermi edge for B at the left-upper side of Fig. 10 is the high-resolution case ($\delta E=95$ meV) and the others are the low-resolution cases ($\delta E=170$ meV). In Fig. 10, the peaks at 0.1–0.3 eV and 2 eV correspond to the final states of f^1 ($4f^2 \rightarrow 4f^1$) and f^0 ($4f^1 \rightarrow 4f^0$), and represent the weight of the f^2 and f^1

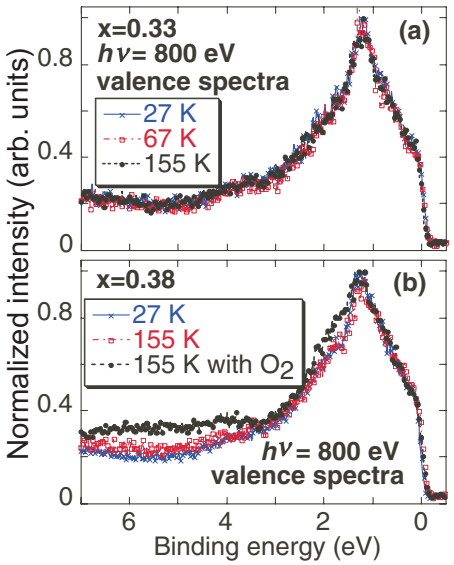

FIG. 9. (Color online) Valence spectra for $x=0.33$ and 0.38 at 27, 67, and 155 K at the incident photon energy of 800 eV.

components in the initial states, respectively. In the high-resolution measurement of Fig. 10, the f^1 peak shows a fine structure, which consists of the $f^1_{7/2}$ (at 0.3 eV) and the $f^1_{5/2}$ (Fermi edge side) components, as observed in other Ce compounds.[47–50] $f^1_{5/2}$ is due to the crystalline electric-field levels and the tail of the Kondo resonance peak. The $f^1_{7/2}$ peak is due to the spin-orbit partner of the tail of the Kondo peak. The intensity of the Kondo resonance peak shows the strength of the c-f hybridization between the $4f$ electrons and conduction band. If there is no c-f hybridization, the f^1 component disappears and only the f^0 component will be seen.[47] Our result shows the existence of the c-f hybridization. If the hybridization strength increases, the Kondo peak intensity will increase accordingly. In Fig. 10 for $x=0.33$, no clear change can be seen in the intensity of f^0 and f^1 when the temperature changes: the change in the intensity is small and higher statistics may be required.

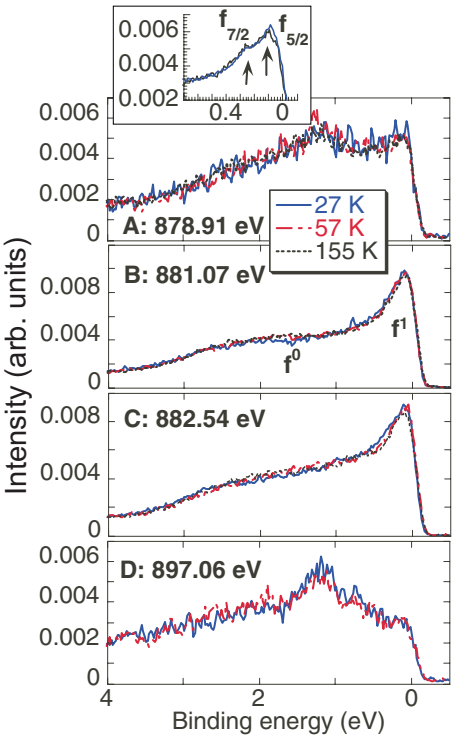

FIG. 10. (Color online) Ce $3d$-$4f$ resonant photoelectron spectra as a function of the temperature for $x=0.33$. The A–E notations correspond to the energies indicated by the arrows in the absorption spectra of Fig. 7. The enlarged spectrum at the left-upper side of the figure is the high-resolution case at the Fermi edge for B.

E. Origin of the valence transition

Adroja *et al.* indicated that a small volume change does not explain the large change in the Kondo temperature, and hence claimed that the KVC model is not applicable.[27] They estimated $\Delta T_K/T_K=6$ and $\Delta V/V=0.003$ for $x=0.35$, where T_K and V are the Kondo temperature and the volume, respectively. Applying these values to the KVC model yields the Grüneisen parameter (Ω) of about 2000 ($\Delta T_K/T_K=-\Omega\Delta V/V$), which is unrealistically large when compared to the case of the transition from γ-Ce to α-Ce ($\Delta T_K/T_K=8.6$, $\Delta V/V=0.14$, and $\Omega=61$). Adroja *et al.* suggested the possibility that the fine tuning of the Fermi-level position could result in a large change in the hybridization and the Kondo temperature with a small change in the volume. A similar scenario was proposed for $YbIn_{1-x}Ag_xCu_4$.[14]

Returning to our measurements, the magnetic susceptibility of the $x=0.33$ sample drops by about 25% at the transition, as shown in Fig. 1. The intensity ratio of f^2 to f^1 and the value of n_f change by a few percent and of the order of 1%, respectively. On the other hand, in the case of the γ-Ce–α-Ce transition, the magnetic susceptibility decreases by more than 70%,[11] about three times more than for $CeNi_{1-x}Co_xSn$ with $x=0.33$. For the intensity ratio of f^2 to f^1, Ce metal shows 15%–50% change, and n_f of the order of 10%.[11,12] These changes are 1 order of magnitude larger than for $CeNi_{1-x}Co_xSn$. This is the reason why most measurements show only a small difference in f^n at the transition in the present study for $x=0.33$. We add the fact that in our measurements the change in the magnetic susceptibility is of the order of 25% around 70 K for the as-cast $x=0.33$ sample: this is smaller than the result obtained by Adroja *et al.*[27] (about 70% for $x=0.35$) and measured with the $x=0.34$ sample (Fig. 1). Our $x=0.34$ sample was not studied with x-ray because of the limitation of the cryostat.

Both resonant x-ray emission and photoelectron spectroscopy suggest a small increase of the valence. The RIXS shows the localized $4f$ states at low temperature. This suggests that the low-temperature state can be understood as a strongly correlated state, where the Kondo effect between the localized $4f$ moment and the conduction electrons play a central role. Therefore, the possibility of the Mott transition model, where the low-temperature state is described by itinerant $4f$ electrons with less electron-electron correlations,[51] should be ruled out.

Finally, we discuss the applicability of the KVC model to our case. In the valence-band RPES spectra, we observed the

Kondo resonance peak (f^1) and the lower Hubbard sideband peak (f^0). For $x=0.33$, the change in the Kondo peak (the strength of the c-f hybridization) is not obvious. This result is in clear contrast to the prediction of the KVC model, where a drastic change in the Kondo peak (f^1) intensity is expected. Such change of the f^1 peak was actually observed in the Ce γ-α transition.[1] Choi *et al.* showed the strong enhancement of the Kondo peak for $CeSi_2$ system when the temperature was decreased.[44] It is noted that in $CeSi_2$ the intensity of the Kondo peak is much stronger than that of $CeNi_{1-x}Co_xSn$, showing weaker Kondo effect in $CeNi_{1-x}Co_xSn$. These results indicate that the Kondo mechanism may play a minor role in $CeNi_{1-x}Co_xSn$. Hence, the KVC model seems unlikely to explain the valence transition of $CeNi_{1-x}Co_xSn$. It is noted that in our other measurements of the RXES and PFY-XAS, we could observe a small change in the initial state of f^2, corresponding to the final state of f^1 in the valence spectra (the Kondo peak) of the PES. Therefore, it is basically difficult to observe such a small change in the valence spectra and there is a possibility that the statistics was not enough.

We recently found the fact that in a similar system, $LaNi_{1-x}Co_xSn$, γ in the specific heat goes through a maximum around the Co concentration with $x=0.38$,[52] where the specific heat (C) is written as a function of temperature (T) as $C(T)=\gamma T+\beta T^2+\delta T^5$ and γ represents the coefficient of the first term. γT is the electronic contribution: the increase of γ corresponds to the increase of the density of states at the Fermi energy. The maximum of γ is roughly correlated with the change in the magnetic behavior. This result suggests the possibility of fine tuning the Fermi-level position as proposed by Adroja *et al.* for $CeNi_{1-x}Co_xSn$. The exact mechanism of the transition, however, is still not clear.

IV. CONCLUSION

The magnetic measurement as a function of the temperature for $CeNi_{1-x}Co_xSn$ confirmed the trend previously shown by Adroja *et al.*[16,27] We performed the x-ray spectroscopic study of photon and electron emissions for $CeNi_{1-x}Co_xSn$ ($x=0.33$ and 0.38). PFY-XAS, RXES, and PES measurements give complementary information on the electronic states. The results clearly demonstrate a sudden change in the Ce valence for the $x=0.33$ sample around 60 K. Resonant inelastic x-ray scattering at the Ce L absorption edge show that the $4f$ state is localized or partially delocalized at 17 K and the degree of hybridization is not strong. The results of PFY and RIXS indicate that the valence transition causes a decrease in the f^1 component and an increase in the f^0 and f^2 components relatively with decreasing temperature.

We have studied the electronic state near the Fermi edge and the temperature variation of f^0 and f^1 by means of the resonant valence-band PES spectra, with nonresonant valence spectra. We observed the Kondo resonance peak (the final state of f^1) in the resonant valence spectra, showing the existence of the c-f hybridization. The change in the intensity of f^1 for $x=0.33$ as a function of the temperature is not clear, although the KVC model expects a drastic change in the Kondo peak. Our other measurements, PFY-XAS and RXES, also indicate a small change in the initial state of f^2 (corresponding to the final state of f^1 in the valence spectra) at low temperature. We add the fact that the estimated Grüneisen parameter by Adroja *et al.* was unrealistic.[27] These results show that the KVC scenario is not likely. Other models such as the Fermi-level tuning due to substitution, as was suggested by Adroja *et al.*,[27] could be considered. Further experimental (for example, PES with higher statistics) and theoretical (including the Fermi-level tuning) studies are still necessary to clarify the origin of the valence transition in the $CeNi_{1-x}Co_xSn$ system.

ACKNOWLEDGMENTS

The experiments were performed at BL15XU (Proposal No. 2005B0159) and BL17SU (BL17 Proposal No. 2005-6) of SPring-8 of the Japan Synchrotron Radiation Research Institute (JASRI). We thank H. Yoshikawa at BL15XU and H. Horiba at BL17SU for help during the experiments. We also deeply appreciate A. Chainani, M. Taguchi, and M. Matsunami in RIKEN, A. Kotani in RIKEN/KEK, and I. Jarrige in JAEA for fruitful discussion.

[1] For a review, see J. W. Allen, J. Phys. Soc. Jpn. **74**, 34 (2005).
[2] J. W. Allen and R. M. Martin, Phys. Rev. Lett. **49**, 1106 (1982).
[3] M. Lavagna, C. Lacroix, and M. Cyrot, Phys. Lett. **90A**, 210 (1982).
[4] J. W. Allen and L. Z. Liu, Phys. Rev. B **46**, 5047 (1992).
[5] L. Z. Liu, J. W. Allen, O. Gunnarsson, N. E. Christensen, and O. K. Andersen, Phys. Rev. B **45**, 8934 (1992).
[6] L. Pauling, J. Chem. Phys. **18**, 145 (1949).
[7] W. H. Zachariasen, Phys. Rev. **76**, 301 (1949).
[8] B. Johansson, Philos. Mag. **30**, 469 (1974).
[9] B. Johansson, I. A. Abrikosov, M. Alden, A. V. Ruban, and H. L. Skriver, Phys. Rev. Lett. **74**, 2335 (1995).
[10] A. K. McMahan, K. Held, and R. T. Scalettar, Phys. Rev. B **67**, 075108 (2003).
[11] J.-P. Rueff, C. F. Hague, J.-M. Mariot, L. Journel, R. Delaunay, J.-P. Kappler, G. Schmerber, A. Derory, N. Jaouen, and G. Krill, Phys. Rev. Lett. **93**, 067402 (2004).
[12] C. Dallera, M. Grioni, A. Palenzona, M. Taguchi, E. Annese, G. Ghiringhelli, A. Tagliaferri, N. B. Brookes, T. Neisius, and L. Braicovich, Phys. Rev. B **70**, 085112 (2004).
[13] I. Felner and I. Nowik, Phys. Rev. B **33**, 617 (1986).
[14] A. L. Cornelius, J. M. Lawrence, J. L. Sarrao, Z. Fisk, M. F. Hundley, G. H. Kwei, J. D. Thompson, C. H. Booth, and F. Bridges, Phys. Rev. B **56**, 7993 (1997).
[15] T. Koyama, M. Matsumoto, S. Wada, and J. L. Sarrao, Phys. Rev. B **63**, 172410 (2001).
[16] D. T. Adroja, B. D. Rainford, J. M. de Teresa, A. del Moral, M. R. Ibarra, and K. S. Knight, Phys. Rev. B **52**, 12790 (1995).

[17] T. Takabatake, F. Teshima, H. Fujii, S. Nishigori, T. Suzuki, T. Fujita, Y. Yamaguchi, J. Sakurai, and D. Jaccard, Phys. Rev. B **41**, 9607 (1990).
[18] T. Takabatake, M. Nagasawa, H. Fujii, G. Kido, M. Nohara, S. Nishigori, T. Suzuki, T. Fujita, R. Helfrich, U. Ahlheim, K. Fraas, C. Geibel, and F. Steglich, Phys. Rev. B **45**, 5740 (1992).
[19] G. Aeppli and Z. Fisk, Comments Condens. Matter Phys. **16**, 155 (1992).
[20] T. J. Sato, H. Kadowaki, H. Yoshizawa, G. Nakamoto, T. Ekino, T. Takabatake, H. Fujii, L. P. Regnault, and Y. Ishikawa, Physica B **223-224**, 432 (1996).
[21] D. T. Adroja and B. D. Rainford, Physica B **199&200**, 498 (1994).
[22] S. Mair, H.-A. Krug von Nidda, M. Lohmann, and A. Loidl, Phys. Rev. B **60**, 16409 (1999).
[23] K. I. Nakamura, Y. Kitaoka, K. Asayama, T. Takabatake, G. Nakamoto, H. Tanaka, and H. Fujii, Phys. Rev. B **53**, 6385 (1996).
[24] D. T. Adroja and B. D. Rainford, J. Magn. Magn. Mater. **135**, 333 (1994).
[25] J. M. De Teresa, D. T. Adroja, B. Rainford, K. S. Knight, A. del Moral, and M. R. Ibarra, Physica B **234-236**, 872 (1997).
[26] K. Kumagai, Y. Furukawa, K. Ooi, B. Rainford, and A. Yakubovskii, Physica B **259**, 294 (1999).
[27] D. T. Adroja, Y. Echizen, T. Takabatake, Y. Matsumoto, T. Suzuki, T. Fujita, and B. D. Rainford, J. Phys.: Condens. Matter **11**, 543 (1999).
[28] A. Nisawa, M. Okui, N. Yagi, T. Mizutani, H. Yoshikawa, and S. Fukushima, Nucl. Instrum. Methods Phys. Res. A **497**, 563 (2003).
[29] D. Horiguchi, K. Yokoi, H. Mizota, S. Sakakura, H. Oohashi, Y. Ito, T. Tochio, A. M. Vlaicu, H. Yoshikawa, S. Fukushima, H. Yamaoka, and T. Shoji, Radiat. Phys. Chem. **75**, 1830 (2006).
[30] H. Yamaoka, M. Taguchi, A. M. Vlaicu, H. Oohashi, Y. Yokoi, D. Horiguchi, T. Tochio, Y. Ito, K. Kawatsura, K. Yamamoto, A. Chainani, S. Shin, M. Shiga, and H. Wada, J. Phys. Soc. Jpn. **75**, 034702 (2006).
[31] H. Tanaka, M. Adachi, T. Aoki, T. Asaka, A. Baron, S. Date, K. Fukami, Y. Furukawa, H. Hanaki, N. Hosoda, T. Ishikawa, H. Kimura, K. Kobayashi, T. Kobayashi, S. Kohara, N. Kumagai, M. Masaki, T. Masuda, S. Matsui, A. Mizuno, T. Nakamura, T. Nakatani, T. Noda, T. Ohata, H. Ohkuma, T. Ohshima, M. Oishi, S. Sasaki, J. Schimizu, M. Shoji, K. Soutome, M. Suzuki, S. Suzuki, Y. Suzuki, S. Takano, M. Takao, T. Takashima, H. Takebe, A. Takeuchi, K. Tamura, R. Tanaka, Y. Tanaka, T. Taniuchi, Y. Taniuchi, K. Tsumaki, A. Yamashita, K. Yanagida, Y. Yoda, H. Yonehara, T. Yorita, M. Yoshioka, and M. Takata, J. Synchrotron Radiat. **13**, 378 (2006).
[32] K. Shirasawa, T. Tanaka, T. Seike, A. Hiraya, and H. Kitamura, AIP Conf. Proc. No. 705 (AIP, New York, 2003), p. 203.
[33] H. Ohashi, Y. Senba, H. Kishimoto, T. Miura, M. Takeuchi, K. Takeshita, S. Goto, S. Takahashi, H. Aoyagi, M. Sano, Y. Furukawa, T. Ohata, T. Matsushita, Y. Ishizawa, S. Taniguchi, Y. Asano, T. Takeuchi, M. Oura, K. Shirasawa, T. Tanaka, Y. Harada, T. Tokushima, K. Horiba, H. Kitamura, T. Ishikawa, and S. Shin, AIP Conf. Proc. No. 523 (AIP, New York, 2007), p. 879.
[34] K. Horiba, N. Kamakura, K. Yamamoto, K. Kobayashi, and S. Shin, J. Electron Spectrosc. Relat. Phenom. **144-147**, 1027 (2005).
[35] H. Ogasawara, A. Kotani, P. Le Fèvre, D. Chandnesris, and H. Magnan, Phys. Rev. B **62**, 7970 (2000).
[36] T. Åberg and B. Crasemann, in *Resonant Anomalous X-ray Scattering Theory and Application*, edited by G. Materlik, C. J. Sparks, and K. Fischer (Elsevier Science, New York, 1994), p. 431.
[37] J.-M. Mariot, J.-J. Gallet, L. Journel, C. F. Hague, W. Felsch, G. Krill, M. Sacchi, J.-P. Kappler, A. Rogalev, and J. Goulon, Physica B **259-261**, 1136 (1999).
[38] C. Dallera, M. Grioni, A. Shukla, G. Vankó, J. L. Sarrao, J.-P. Rueff, and D. L. Cox, Phys. Rev. Lett. **88**, 196403 (2002).
[39] L. Journel, J.-M. Mariot, J.-P. Rueff, C. F. Hague, G. Krill, M. Nakazawa, A. Kotani, A. Rogalev, F. Wilhelm, J.-P. Kappler, and G. Schmerber, Phys. Rev. B **66**, 045106 (2002).
[40] H. Yamaoka, M. Oura, M. Taguchi, T. Morikawa, K. Takahiro, A. Terai, K. Kawatsura, A. M. Vlaic, Y. Ito, and T. Mukoyama, J. Phys. Soc. Jpn. **73**, 3182 (2004).
[41] T. K. Sham, R. A. Gordon, and S. M. Heald, Phys. Rev. B **72**, 035113 (2005).
[42] E. Annese, J.-P. Rueff, G. Vankó, M. Grioni, L. Braicovich, L. Degiorgi, R. Gusmeroli, and C. Dallera, Phys. Rev. B **70**, 075117 (2004).
[43] J.-P. Rueff, L. Journel, P.-E. Petit, and F. Farges, Phys. Rev. B **69**, 235107 (2004).
[44] B.-H. Choi, R.-J. Jung, S.-J. Oh, E.-J. Cho, T. Iwasaki, A. Sekiyama, S. Imada, S. Suga, T. Muro, and Y. S. Kwon, J. Electron Spectrosc. Relat. Phenom. **136**, 15 (2004).
[45] O. Gunnarsson and K. Schönhammer, Phys. Rev. B **28**, 4315 (1983).
[46] J. C. Fuggle, F. U. Hillebrecht, Z. Zolnierek, R. Lasser, C. Freiburg, O. Gunnarsson, and K. Schönhammer, Phys. Rev. B **27**, 7330 (1983).
[47] F. Patthey, J.-M. Imer, W.-D. Schneider, H. Beck, Y. Baer, and B. Delley, Phys. Rev. B **42**, 8864 (1990).
[48] A. Sekiyama, K. Kadono, K. Matsuda, T. Iwasaki, S. Ueda, S. Imada, S. Suga, R. Settai, H. Azuma, Y. Onuki, and Y. Saitoh, J. Phys. Soc. Jpn. **69**, 2771 (2000).
[49] A. Sekiyama, S. Suga, T. Iwasaki, S. Ueda, S. Imada, Y. Saitoh, T. Yoshino, D. T. Adroja, and T. Takabatake, J. Electron Spectrosc. Relat. Phenom. **114-116**, 699 (2001).
[50] A. Sekiyama and S. Suga, Physica B **312-313**, 634 (2002).
[51] A. Kotani and H. Ogasawara, J. Electron Spectrosc. Relat. Phenom. **60**, 257 (1992).
[52] N. Tsujii *et al.* (unpublished).